iScience

CellPress
OPEN ACCESS

Article

Climatic and tectonic significance of Taboche Lake, Khumbu Region, Nepal

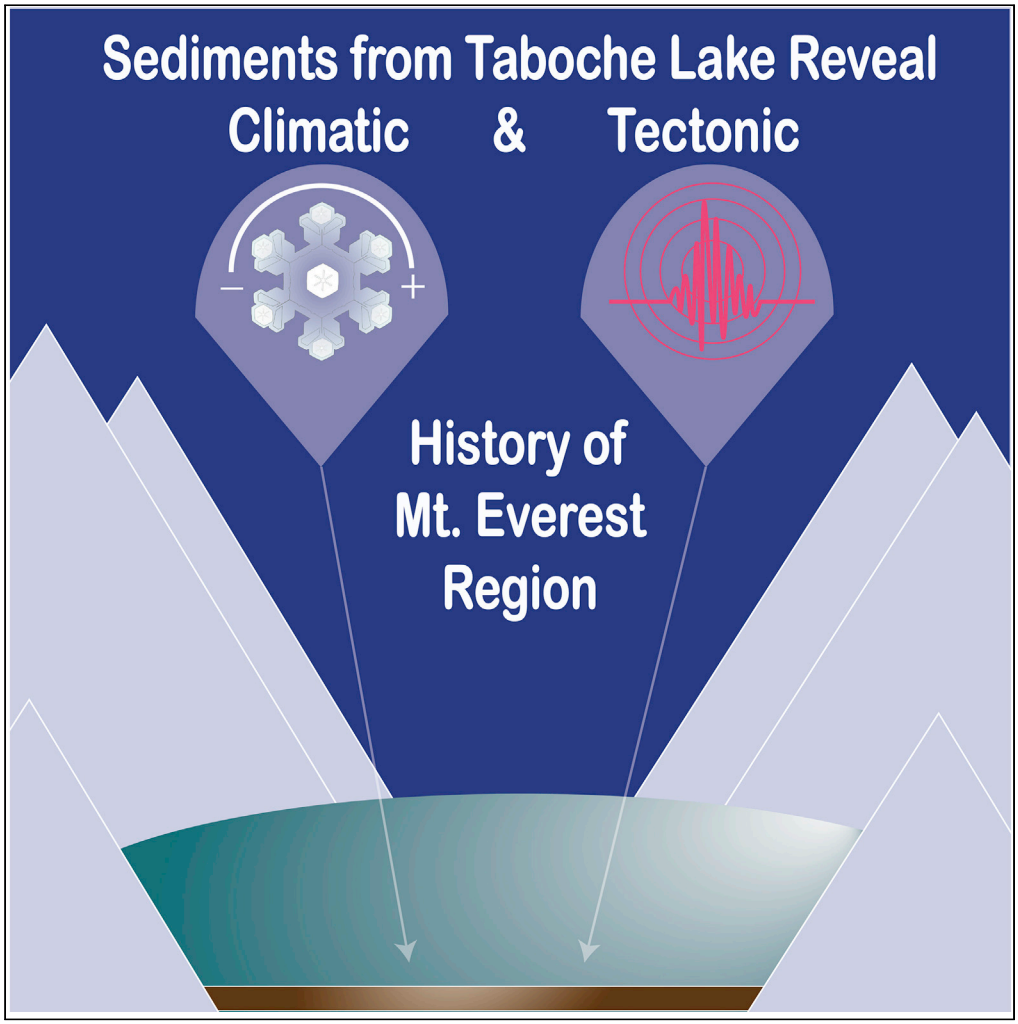

Ananta P. Gajurel, Mary S. Hubbard, Bibek Giri, ..., Sandra Elvin, Alex Tait, Paul A. Mayewski

apgajurel@fulbrightmail.org

Highlights

Sedimentology and dating are essential to identify environmental changes in lake cores

Post-1807 AD ± 112 years flood turbidite record indicates warming trend in the Himalaya

Earthquake-triggered turbidite and slump event in the core relate to historic tremors

Earthquake records in glacial lake core highlight tectonic risk, which can cause GLFs

Gajurel et al., iScience *24*, 102418
May 21, 2021
https://doi.org/10.1016/j.isci.2021.102418

iScience

CellPress
OPEN ACCESS

Article

Climatic and tectonic significance of Taboche Lake, Khumbu Region, Nepal

Ananta P. Gajurel,[1,7,*] Mary S. Hubbard,[2] Bibek Giri,[2] Aurora C. Elmore,[3] Sanjeet Maka,[1] Patrick A. Rafter,[4] Aaron E. Putnam,[5,6] Sandra Elvin,[3] Alex Tait,[3] and Paul A. Mayewski[5]

SUMMARY

The Everest region is characterized by its alpine glacial environment. In an effort to understand environmental change and tectonic activity, our team cored Taboche Lake, situated at 4,712 m along the western margin of the Ngozumpa Glacier. This research catalogs past earthquakes using geological records of the lake core that are important for the assessment of future earthquake hazards in the region and provides information for tectonic risk of glacial lake floods. Core grain size characteristics and internal sedimentary structures from computed tomographic scan were coupled with radiocarbon dating of organic matter preserved in the core to reconstruct the environmental history of the area. The 58-cm-long core consists of laminated silty sands and sandy silts with particle diameters <2 mm. The core records a syn-sedimentary deformational structure, folded sediments, rhythmically alternating dark- and light-colored laminations, and turbidites, which indicate coeval climatic and tectonic variations over the past ~1,600 years.

INTRODUCTION

The transect across the Himalayan mountain range from the southern plains at elevations less than 100 m above mean sea level to the region over 8,000 m in Nepal is around 150 km in width, and within this transect a wide range of climatic conditions prevail. Climatic zoning is complex, and the environment is highly sensitive to climate change (Karki et al., 2015). High elevation areas in the region near Mt. Everest (known locally as Sagarmatha in Nepal and Qomolangma in China) are characterized by a glacial environment. Glaciers have responded to climatic warming in many ways—lowering glacial surfaces, forming lakes, and ultimately decreasing the aerial extent of glaciers in the Mt. Everest region by 5% during the second half of the 20th century (Shrestha et al., 1999; Rowan et al., 2015; Shea et al., 2015; King et al., 2017, 2018). Supraglacial debris and moraine deposits are the main sources of sediment during flooding events such as the sudden draining of lakes due to destabilization of the glacial system, either by climate change or tectonic activity (ICIMOD, 2011; Benn et al., 2012; Byers et al., 2017; Liu et al., 2020). Such events can trigger flood hazards to downstream settlements and infrastructure (Richardson and Reynolds, 2000; Benn et al., 2001). Thus, the impact of climate change on high mountain environments is critical to the understanding of glacial hazard assessment and risk reduction processes as well as monitoring the availability of water resources to the population living in downstream valleys and plains. Similarly, ongoing tectonic activity in the Himalayan-Tibetan terrain challenges the stability of high-altitude glacial lakes.

The Ngozumpa Glacier is the longest glacier in the Khumbu region—descending from Cho Oyu (8,188 m) in the west, and No Jumba Kan (7,743 m), Gyachung Kang (7,861 m), Hunchhi (7,029 m), and an unnamed 6,286 m peak in the east—forming a clean glacier surface above 5,250 m with extensive debris cover downglacier (Benn et al., 2017). In an effort to understand environmental change and tectonic activity in the area, our team cored the Taboche or "Second Lake" situated at 4,712 m along the western margin of the lateral moraine of the Ngozumpa Glacier. Locations of sampling sites are illustrated in Figure 1. Moraine and outwash deposits surrounding the lake are sporadically covered by grass and bushes. Lichen-coated boulders constitute the majority of outwash alluvial fan deposits debouched from Ngozumpa Glacier eroding across the western lateral moraine dam (Figure 2).

The Himalaya region is seismically active because of continuous subduction of the Indian plate at a rate of ~20 mm/year beneath the Asian plate (Jackson and Bilham, 1994; Zheng et al., 2017). The Khumbu region

[1]Department of Geology, Tribhuvan University, Kathmandu, Nepal

[2]Department of Earth Sciences, Montana State University, Bozeman, MT, USA

[3]National Geographic Society, Washington, DC, USA

[4]University of California, Irvine, CA, USA

[5]Climate Change Institute, University of Maine, Orono, ME, USA

[6]School of Earth and Climate Sciences, University of Maine, Orono, ME, USA

[7]Lead contact

*Correspondence: apgajurel@fulbrightmail.org

https://doi.org/10.1016/j.isci.2021.102418

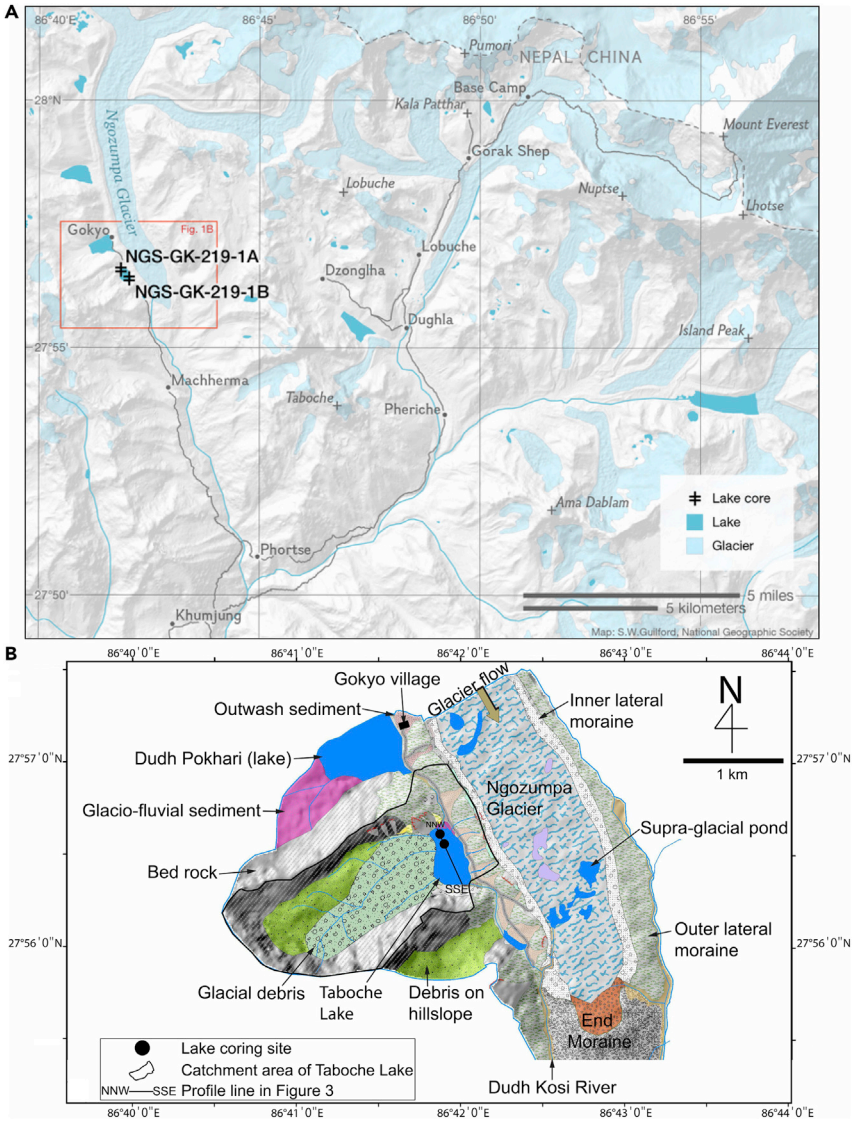

Figure 1. Location of lake coring sites situated in the Gokyo valley

(A) The regional map shows the Khumbu region and Mt. Everest, the Gokyo Valley, and lake core locations on Taboche Lake, as well as the other regional lakes (aqua) and glaciers (light blue), along with the main trekking route (gray lines) and river systems (blue lines) as well as village names (circles) and major peaks (crosses). The locations of inset maps are shown by red boxes.

(B) Geomorphological map of the Taboche Lake area depicting various geomorphological elements and the location of the two cores in Taboche Lake (circles). The catchment area for the Taboche Lake (black outline) is shown according to the Nepal Survey Department (Survey Department, 1996).

has experienced several great ($M \geq 8$) and major ($7 \geq M < 8$) earthquakes in the recent past, including six major and four great earthquakes since 1100 (Bilham, 2019). Earthquakes are a major natural hazard in the Nepal Himalaya. Knowing the past historical earthquake record provides insight for future recurrence of great earthquakes in the Himalaya. Lake sediments are good geological archives of past major and great earthquakes (Gajurel et al., 1998; Ghazoui et al., 2019; Vandekerkhove et al., 2020). Therefore, cataloging past earthquakes from either historical or geological records is important for assessment of earthquake hazards in the region. Although evidence of earthquakes is geographically widespread and thus cores to reconstruct tectonic activity could have been collected from lower elevations, knowing the climate variability (i.e., warming or cooling trends), especially at high elevations, is crucial knowledge for planning to cope with hydro-meteorology-related hazards. Thus, for the climatic reconstructions, our cores were

Figure 2. Proximal regional setting for Taboche Lake

Drone photograph showing the shore of Taboche Lake, its surrounding area to the north, and highlighting select geologic characteristics in yellow text. A corner of Dudh Pokhari (Third Lake) can also be seen in the background, which provides some overflow into Taboche Lake. (Photograph credit: Brittany Mumma/National Geographic).

collected at the highest elevations possible for our expedition team. Evaluation of sediment characteristics and structural variability in lake cores recovered from the glacial environment is important to establish proxies that are related to environmental change and/or tectonic activity. Tectonic activity related to ground shaking motion is indicated by liquefaction and fluidization structures in sediments (Sims, 2012; Nakashima and Komatsubara, 2016).

The watershed of Taboche Lake is bound by a 1.25-km-long, northwest-southeast trending ridge consisting of a peak called Phari Lapche (6,017 m) that trends in a southwest direction from the lake and a nearly parallel spur 1.25 km to the north (Figure 1B). The Taboche Lake is part of the Gokyo Lake system, the world's highest oligotrophic freshwater lake system (Lin et al., 2018), which is located around 15 km from Mt. Everest. The northeast side of the lake is demarcated by the western lateral moraine slope of the Ngozumpa Glacier. Taboche Lake, with a catchment area of 3.3 km^2 and a perimeter of 8.91 km, is developed at the terminus of a paleo-glacier that covers an area of 0.8 km^2 with a perimeter of 4.3 km descending toward east-northeast from the Phari Lapche peak (Figure 1B). The catchment area of the study lake consists of terrain with predominantly less than 45° slopes that are dominantly north to northeast facing and a small proportion of slopes that are facing toward southeast, southwest, and northwest. Small streams appear in the U-shaped northeast sloping valley at the southwestern watershed area of the lake. The lake is also fed by overflow from the Dudh Pokhari (Third Lake), located next to Gokyo village (Figure 1B). The bedrock consists of schist and gneissic rock with granitic pegmatites and migmatites (Hubbard, 1989). Taboche Lake is a moraine-dammed lake located along the western margin of the lateral moraine of Ngozumpa glacier, which covers a small catchment area consisting mostly of glacial debris cover and a small area of basement rock exposure that has scree deposits, which are the major extraformational sediment sources to the lacustrine sedimentation in the Taboche Lake (Figure 1B). The extra-formational sediments are transported mainly by the action of glaciers and surface water. The present-day basin setting shows that surface runoff is the main sediment transporting agent into the lake; however, rock fall/slumping processes also contribute sediments into the lake from surrounding hillslopes. Quantification of the sediment contribution of these transporting agents has not yet been done in the area.

Two cores, NGS-GK-219-1A (27.94289 °N, 86.698232 °E) and NGS-GK-219-1B (27.941853 °N, 86.698747 °E), were collected from Taboche Lake to assess changes to this high elevation Gokyo Valley environment through time (Figures 1 and 3). For core NGS-GK-219-1A, we used computed tomographic (CT) scanning to better resolve structural deformation. Discrete samples were subsequently taken for grain size analysis to resolve environmental changes and for radiocarbon (^{14}C) dating to generate a chronology. A full

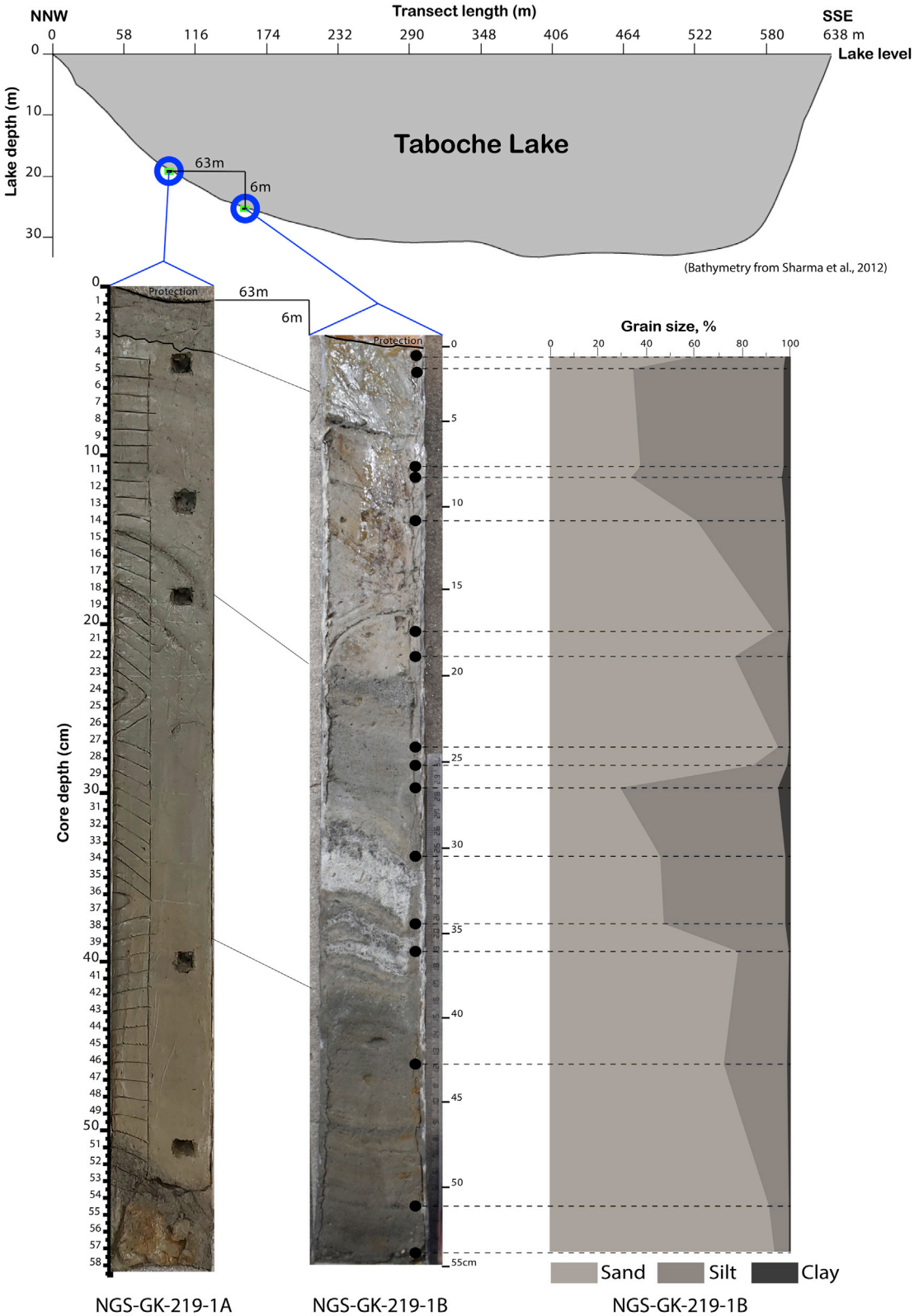
NNW
SSE
Transect length (m)
0
58
116
174
232
290
348
406
464
522
580
638 m
Lake level
Lake depth (m)
Taboche Lake
63m
6m
(Bathymetry from Sharma et al., 2012)
Protection
Core depth (cm)
Grain size, %
0
20
40
60
80
100
55cm
Sand
Silt
Clay
NGS-GK-219-1A
NGS-GK-219-1B
NGS-GK-219-1B

Figure 3. Location and description of the Taboche Lake cores

Position and photographs of cores NGS-GK-219-1A and NGS-GK-219-1B in Taboche Lake are shown with the lake's bathymetry at the top, lithological correlation. Grain size distribution with respect to depth from core NGS-GK-219-1B is shown to the right side of the figure, and the data are available in Table S1.

description of our methodology can be found in the Experimental Procedures section. Our major research questions were: (1) what could be the cause of the folded structure preserved in core NGS-GK-219-1A and (2) do the Taboche Lake cores reflect climate/environmental changes (e.g., slumping due to flooding) or are they an indicator of a significant tectonic event in the Himalaya? In this article we examine the sediments and sedimentary structures of the lake cores recovered from Taboche Lake in an effort to understand past environmental changes in this high-mountain area of the Himalayas. Our geologic observations coupled with ^{14}C radiometric ages allow us to better understand hydro-meteorology-related hazards and related geological hazards in the Himalaya.

RESULTS

Lake core lithology and sediment characteristics

Core lithological description is given in Figure 4, and the textural name for mixtures of sand, silt, and clay is defined according to Folk (1980) in Figure 5. The lithology of core NGS-GK-119-1A is composed of light to dark gray silty sands with silty laminae, light gray sandy silts with sandy laminae, and tan and blackish silts with sandy laminae in the upper half of the core, whereas the lower half of the core consists predominantly of blackish, brownish to gray silts having sandy laminae and a 5-cm-thick layer of fine micaceous sandy sediments at the bottom of the core. The lower half of the core shows a relatively higher proportion of coarse organic debris than in the upper part (Figure 4). Sporadic very coarse sand size fragments of quartz are found between 40 and 45 cm depth of the core in silty materials during visual inspection.

For the second core, NGS-GK-119-1B, the lithology is composed of light gray sandy silts and silty sands with sandy and silty laminae in the upper half and the lower half consists of light to dark gray sandy silts to silty sands with sandy and silty laminae. Grain size analyses reveal that particle diameter of the sediments are less than 2 mm. Five sediment samples reveal particle sizes $\leq$1.9 mm in diameter. Six sediment samples have only particles $\leq$0.295 mm in diameter, whereas the remaining samples contain particles that range in size between 0.295 and 1.9 mm, with some smaller sizes. The proportions of sand- (0.062–2 mm), silt- (0.002–0.062 mm) and clay-size (<0.002 mm) particle distribution range from 29.5% to 95%, 65% to 4.2%, and 0.4% to 5.5%, respectively (Figure 3 and Table S1). The sand-silt-clay ternary diagram in Figure 5 shows the presence of a lower proportion of clay ($\leq$1.9%) in the sediments located toward the apex of the sand size field than the sediments distributed toward the silt size field (clay $\leq$5.5%). This distribution indicates that a variation in the relative energy from higher current to lower current conditions can be assumed at the same site of sedimentation over time in the lake. The proportion of sand from 61% to 95% is found between 24.5 and 10 cm depth of the core. Likewise, the proportion of sand is high (72%–93%) between 35 and 56 cm sediment depth. Silt ranges from 50% to 65% between 25 and 35 cm core depth. The upper 7.5 cm of the core is rich in silt sediment (~60%) except for a very thin, silty sand layer at the top.

Lake core chronology

Six sediment samples at 4–5 cm, 8–9 cm, 12–13 cm, 18–19 cm, 39.5–40.5 cm, and 50.5–51.5 cm depth of core NGS-GK-219-1A were analyzed for ^{14}C dating (Figure 4 and Table 1). Among the six samples measured from core NGS-GK-219-1A, the youngest age found is 85 BP $\pm$ 25 years corresponding to 95.4% probability age in calendar years as 1807 AD $\pm$ 112 years at 12–13 cm core depth, which is probably out of the calibration range. Sediments at 50.5–51.5 cm depth produced 1795 BP $\pm$ 15 years, with a 95.4% probability age in calendar years as 228.5 AD $\pm$ 91.5 years. Thus, the 58-cm-long core records up to ~1,600 years of sedimentation in the lake.

We should note that several studies of Tibetan Plateau lake water radiocarbon report surface water ^{14}C ages that are older than modern (e.g., Mischke et al., 2013). This "reservoir age" observed in some Tibetan Plateau lakes is acquired from the addition of carbon from ^{14}C-depleted carbonate (older than 50,000 years BP) to the watershed feeding a lake. In the absence of comparable measurements of surface lake water from our sites (or within a reasonable distance from our site), it is difficult to determine the reservoir age for our study. Furthermore, it is possible that the mineralogy of the local watershed (primarily quartz and feldspar [Hubbard, 1989; Casey et al., 2012]) precludes a significant influence of ^{14}C-depleted carbon on

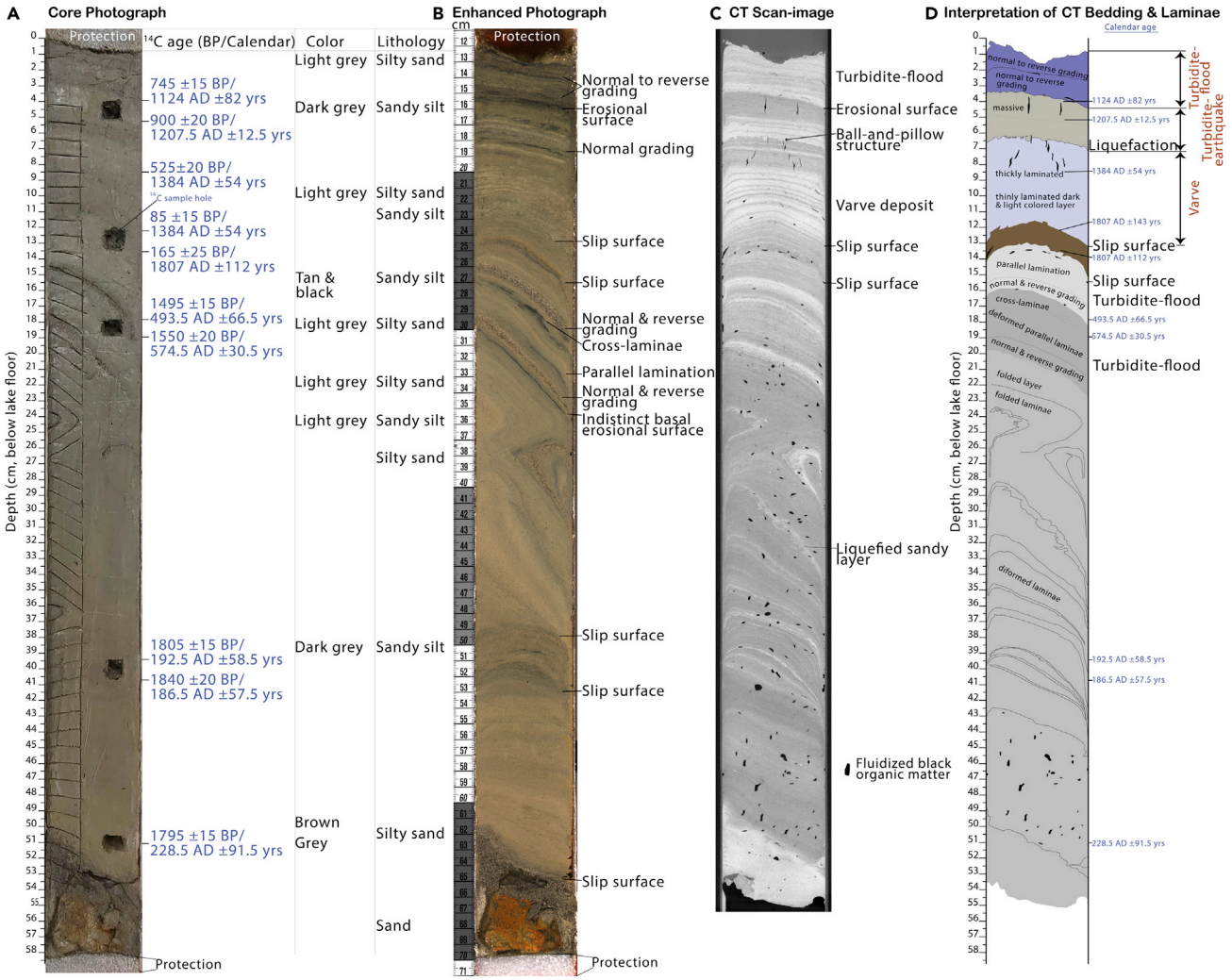

Figure 4. Cross-sectional image of a core from Taboche Lake

(A) Photograph of lake core NGS-GK-219-1A with lithological description and ^{14}C age.

(B–D) (B) Enhanced photograph depicting various sedimentary features from core NGS-GK-219-1A. (C) CT scan image of core NGS-GK-219-1A. (D) Interpretation of CT bedding and laminae with position of ^{14}C age for NGS-GK-219-1A (^{14}C data is shown in Table 1).

Taboche Lake water ^{14}C ages. Finally, the fact that we observe relatively young ^{14}C ages (e.g., 85 ± 15 years BP) argues against a dramatically old lake water ^{14}C reservoir age at this site. As such, we have not incorporated a reservoir age into our age model. Furthermore, another important caveat to using bulk sediment organic matter ^{14}C ages to constrain the age model is the likelihood of biasing toward older ^{14}C, and therefore calendar ages, via the introduction of ^{14}C-depleted organic carbon.

Depositional and deformational structures

Recognition of depositional, erosional, and syn-sedimentary deformational structures in sedimentary packages is crucial to get sedimentation history and associated activity in the depositional basin. First, attempts were made to distinguish structural packages that are preserving *in situ* depositional environmental factors for the explanation of sedimentation processes, such as the depositional environment with respect to relative energy strength, including for transportation and deposition of sediments within the lake. Core NGS-GK-219-1A shows depositional, erosional, and deformational structures. Depositional structures are characterized by parallel and cross-laminae and graded bedding that developed during sedimentation processes of sandy and silty sediments in the lake. Thin to thick lamina is formed by sandy and silty sediments. Rhythmically alternating dark- and light-colored laminations formed in the lake core

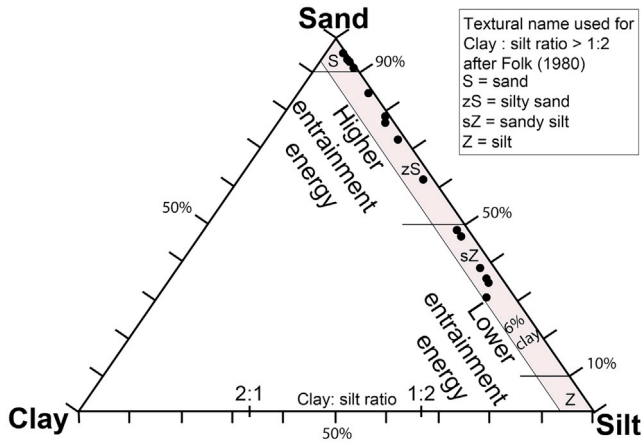

Figure 5. Sediment grain size of Taboche Lake core samples

Ternary mixing diagram showing the relative proportions of sand, silt, and clay size sediments from core NGS-GK-219-1B shows the presence of clay size fragments (<2 μm) less than 6% in the sediments, with most samples being more sandy than silty.

NGS-GK-219-1A between 6 and 12 cm sediment depth could be the result of seasonal variations in sediment flux into the lake. Such dark- and light-colored couplets are consistent with annual varve deposits (Larsen et al., 2011).

Graded structure is produced in sedimentary deposits by changes in grain sizes, with fining upward sections termed as "normal" and coarsening upward sections called "inverse" grading. These structures are produced by changes in size of sandy and silty particles. Between 13 and 20 cm depth in core NGS-GK-219-1A, there are normal to inversely graded sandy layers with an erosional basal surface that evolves upward to a parallel-laminated, silty-sandy layer, which further changes up-section to a cross-laminated silty layer; these characteristics belong to a typical turbidite deposit in the lake (Figure 4).

There are a few specific sedimentological features among the otherwise laminated sediment, the micro-scale ball-and-pillow structure on the sole of a sandy layer found at 6.5 cm in core NGS-GK-219-1A is a kind of syn-sedimentary deformational structure. Several slip surfaces are detected in core NGS-GK-219-1A and are characterized by micro-scale fragmentation of silty-sandy sediments and disrupted lamination in silty-sandy sediments, corresponding to a slumping event. Folding of sediments is evident between 20 and 38 cm in core NGS-GK-219-1A. Sandy and silty layers are folded into an inclined "z"-type pattern (Figure 4). Upper and lower limbs of the "z" fold are higher in dip amount than the middle limb. The top covering sediments in core NGS-GK-219-1A are characterized by two sets of normal graded layers. The basal sedimentation unit starts from sandy particles on an erosional basal surface that gradually fines up section, revealing indistinct parallel lamination in a silty sediment layer.

DISCUSSION

Sediments in the Taboche Lake cores were examined to understand the sedimentary processes during the deposition period of the 58-cm-thick sediment section to reconstruct the paleo-environment and for detection of major earthquake activity over the time. Core NGS-GK-219-1A shows noticeable folding structures, whereas core NGS-GK-219-1B, located further toward the basin's center, does not show such structures. Additionally, the explanation of a 9-cm-long sediment core recovered from a deeper part of the same basin at about 175 m south of the site of this study by Sharma et al. (2012) did not exhibit deformational structures. ^{14}C ages of core NGS-GK-219-1A, together with depositional sedimentary structures that are preserved *in situ* are important for the interpretation of sedimentary processes during depositional times in Taboche Lake. Because we observe slumping structures, we know that there may have been some mixing in the older sediments. The ^{14}C ages of this study are therefore critical to identifying the extent of this mixing.

To further understand the ages of our cores, we correlated them to sediment from Lower Pyramid Lake in the Mt. Everest region, as described in Lami et al. (2010) to resolve age reversals seen in this study.

Table 1. Lake core chronology

Depth in core (cm)	^{14}C age (BP)	Converted calendric age (AD ± yrs)
4–5	900 ± 20	1124 ± 82
	745 ± 15	1270.5 ± 12.5
8–9	525 ± 20	1384 ± 54
12–13	165 ± 25	1664
	85 ± 15	1807 ± 112
18–19	1550 ± 20	493.5 ± 66.5
	1495 ± 15	574.5 ± 30.5
39.5–40.5	1805 ± 15	192.5 ± 58.5
	1840 ± 20	186.5 ± 57.5
50.5–51.5	1795 ± 15	228.5 ± 91.5

^{14}C age data for the first Taboche Lake core, NGS-GK-219-1A.

Deviation of a minimum of 160 years between the two lakes' sediment in ^{14}C age at 40–41 cm depth and positioning the measured ages of both lake sediments at 18–19 cm depth within the ^{14}C age range indicates that sediments of Taboche Lake and Lower Pyramid Lake are very closely correlated with respect to depositional age and therefore, rates of deposition. In contrast, sediments dated at 12–13 cm depth of Taboche Lake that are confined between upper and lower slip surfaces correspond to displaced sediments due to a slumping event from its original stratigraphic position. Thus, the order of superposition of sediments in core NGS-GK-219-1A is disturbed from 13-cm-depth up-section. We discuss here the characteristic features observed in the sediments with their significance starting with the deeper part of the cores.

The basal section of core NGS-GK-219-1A at around 50–53 cm depth has a slip surface where coarser sandy sediments are intruded into finer sandy-silty sediments within a narrow depth interval. Above the slip surface, the long axes of black organic debris particles are oriented nearly parallel to the length of the core, which could be a result of fluidization processes affecting this 5-cm-thick section. These processes could be associated with a slumping event (Figure 4).

The presence of a slip surface at ~ 38 cm of core NGS-GK-219-1A distinguishes the upper boundary of coarser materials (sand) from the overlying, steeply inclined sedimentary layers. Sandy sediments appear between 58 cm and 38 cm depth in the core. Dates determined for core NGS-GK-219-1A in this interval (50.5–51.5 cm depth [228.5 AD ± 91.5 years] and 39.5–40.5 cm depth [192.5 AD ±58.5 years and 186.5 ± 57.5 years]) correspond to a warm period with a reduced ice cover in the Mt. Everest region (Lami et al., 2010). Warmer conditions are corroborated by the presence of dark organic debris and the higher proportion of coarse sediments (sands) that support the existence of higher energy transport into the lake. The high proportion of sand (93–72%) between 35 and 56 cm of our other core, NGS-GK-219-1B, is also consistent with sand transportation via high water-current energy (Figure 5).

Sediments in core NGS-GK-219-1B from 20 to 38 cm depth correspond to a zone of folded layers in core NGS-GK-219-1A that oscillate between coarse and fine sediments with embedded organic debris. This alternation indicates a variation in current strength in transport energy into the lake. Lami et al. (2010) suggested oscillations between colder and relatively warmer phases for the period between 300 and 900 AD in the region, which could be the cause of our alternating layers of coarse and fine sediment in that interval.

In core NGS-GK-219-1A, the interval between 14 and 20 cm has two sediment sequences that are characterized by small-scale graded bedding that evolve up-section to parallel laminated silty sands and cross-laminated silty sediments. This configuration is characteristic of fine-grained turbidite deposits (Stow and Shanmugam, 1980). The origin of the turbidite deposit could either be from a flood or an earthquake Ghazoui et al. (2019); Vandekerkhove et al. (2020), although several workers prefer a flood interpretation for this type of deposit (Beck, 2009; Vanniere et al., 2013; Sabatier et al., 2017). These sediments were deposited into the lake by turbidity currents with high enough entrainment energy to carry sandy material, which is equivalent to the central portion of the core NGS-GK-219-1B, where the fining up-section grain size

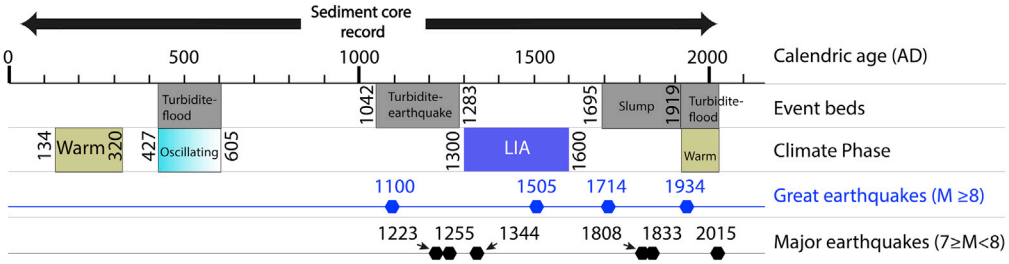

Figure 6. Great and major seismic events in the Himalaya

A linear diagram showing ^{14}C calendric age in AD of lake core sediments together with a catalog of great and major earthquakes in Nepal (middle west, central, and east) and Bhutan. Key markers and milestones, such as the Little Ice Age in the Himalaya are also included to show alignment with the composition of the lake cores.

distribution is evident (Figure 3). Depositional age of the sediments is found to be 574.5 AD ± 30.5 years/ 493.5 AD ± 66.5 years from radiogenic carbon dating at 18–19 cm depth. Oscillations between colder and relatively warmer phases are identified between 300 and 900 AD in the Mt. Everest region from core pigments and diatoms found in nearby Lower Pyramid Lake (Lami et al., 2010). Thus, these turbidite units could be developed in Taboche Lake by heavy precipitation, high meltwater flux, or runoff discharge. Moreover, distribution of sands is found in higher proportion (61%–95%) between 10 and 24.5 cm sediment depth of core NGS-GK-119-1B, where clay size fragments are lower in proportion (Figure 5), suggesting transport energy conditions were higher and sedimentation of clay was not favorable.

There is a 1-cm-thick layer of fine-grained sediment (silts) situated at the core interval between 12 and 13 cm depth that is bounded on top and bottom by slip surfaces. These sediments consist of light gray silts with mica. The depositional age of the sediment is 1807 AD ± 112 years. The age of the overlying 4 cm (considering 3 cm top cover plus 1 cm between the slip surfaces) could be comparable to the Lower Pyramid Lake section at 6–7 cm depth that was dated at 1880 AD (Lami et al., 2010). Thus, slumping was triggered during the upper age limit of sedimentation, ~1919 AD in the Taboche Lake deposits. Between the time frame of 1695 and 1919 AD, sedimentary units do not show any turbidity current-related sedimentation process regulated by heavy flooding. Moreover, these sediments do not contain extra-formational clasts greater than 2 mm in diameter, which rules out the possibility of landslide input originating from the hillslopes at the western and northwestern periphery of the lake.

Interestingly, folded layers in an inclined "Z"-shaped pattern from 12 to 38 cm depth illustrate a converging direction, which we interpret to indicate the transport direction from source to depositional area. This mass transport deposit is likely the product of a slumping event in the lake. The timing of this event lies within the time frame of great earthquakes ($M \geq 8$) that occurred in 1714 AD in Bhutan and in 1934 AD in Nepal, as well as other major Himalayan earthquakes ($7 \geq M < 8$) that happened in central Nepal in 1808 or 1833 AD (Figure 6). The inclined sandy liquefied layer at the depth interval between 29 and 34 cm (Figure 4C) further attests to slumping that could have been associated with an earthquake event.

Like the "Z"-shaped fold, we interpret the 3-cm-thick turbidite deposit with a distinct erosive base at core interval from 3.5 to 6.5 cm as an earthquake-triggered event (Ghazoui et al., 2019; Vandekerkhove et al., 2020). Grain size distribution patterns show a fining up-section from sand to silt grade in core NGS-GK-219-1B. ^{14}C age range of the sediment in core NGS-GK-219-1A varies from 1042 to 1283 AD at 4–5 cm depth and corresponds to the great medieval earthquake ~M 8.8 that hit in ~1100 AD in central Nepal (Lavé et al., 2005) or to historical earthquakes in 1223 or 1255 AD (Pant, 2002). Microscale ball-and-pillow structure at 6.5 cm depth of core NGS-GK-219-1A (Figure 4) developed due to liquefaction of sandy materials (Sims, 1973) could have been triggered by the strong aftershocks of the earthquake in the region. Moreover, vertical orientation of organic debris close to the microscale ball-and-pillow structure suggests the occurrence of fluidization process at increased pore water pressure conditions within the sediments associated with transformation of seismic energy.

The uppermost sediment cover of the lake might have been disturbed during the coring process; however, the uppermost 3-cm-thick sediment in core NGS-GK-219-1A represents turbidite beds that corresponds to the post-1807 AD ± 112 years (Figure 6). This means that these sediments were deposited after a climatic

event called the Little Ice Age (LIA). In the Himalaya, the LIA ranges from 1300 to 1600 AD (Rowan, 2017) and glacier surfaces during the LIA reached to the maximum height of present-day lateral moraine ridges (Sakai and Fujita, 2010). In contrast, the last glacial advances of the LIA occurred around 200 years ago in Tian Shan (Li et al., 2017). The characteristics of the turbidite indicate an origin associated with floods due to heavy precipitation, summer ice or snow melt, or breaching of perched lakes developed above the englacial base-level on impermeable Ngozumpa Glacier ice close to the lake (Benn et al., 2012) across the western lateral moraine, which left coarse outwash debris as an alluvial fan-shaped deposit on lateral moraine slope (Figure 1B; 2). The fines could have been transported into the lake at a higher current energy associated with warming in the Himalaya after the end of the LIA.

Since the 1950s, new lakes in the glacierized Himalayan regions of Nepal have been developing and increasing their volumes owing to accelerated glacier retreat and glacial surface lowering caused by the increasing temperature trend (0.086°C/year) at higher altitudes (Shrestha et al., 1999; Benn et al., 2001; Bajracharya and Mool, 2009; Somos-Valenzuela et al., 2015; DHM, 2017; Khadka et al., 2018). Recently, Bajracharya et al. (2020) have identified 2,070 glacial lakes in Nepal and found a 24% reduction in the glacial area between 1977 and 2010 AD. They also found that most of the glacial lakes are situated between 4,000 and 6,000 m altitude, ranging in size from 0.2 to 5 km^2. In the Everest region, modeled glacier area change between 1961 and 2007 decreased ~20% (Shea et al., 2015). From 1987 to 2017, surface area of glacial lakes expanded up to ~25% (Khadka et al., 2018). Among these glacial lakes, 47 in the Nepali Himalaya are categorized as potentially dangerous (Rounce et al., 2017; Bajracharya et al., 2020). The Kosi river basin incorporates 42 of these lakes, which creates a high risk to the populations living downstream in both Nepal and India (Ghimire, 2004). For example, a glacial lake flood (GLF) in 1985 from Dig Tsho Lake, located to about 13 km southwest of this study area caused significant economic loss (USD 1.5 million) and resulted in lives lost downstream (Vuichard and Zimmermann, 1986; Mool et al., 2001; Horstmann, 2004). In fact, over the past five decades, 26 GLF events that originated in Nepal and Tibet have caused significant damage to lives, livelihoods, and property (Rana et al., 2000; Bajracharya et al., 2020).

In addition to climatic impact on the stability of glacial lake dams, instability of moraine dams in the Mt. Everest region was augmented by the M 7.8 Gorkha earthquake and its aftershocks in 2015 (Byers, et al., 2017). Data of past earthquake records in the High Himalaya are critical to assess the earthquake-triggered GLF hazard to the downstream population and infrastructures in Nepal and India, especially because downstream social, environmental, and economic threats due to GLFs could be massive (Shrestha et al., 2010; Somos-Valenzuela et al., 2015). Recent scientific research indicates that elastic strain energy has been stored at the décollement near the transition between aseismic and co-seismic slip zones of Indo-Tibetan convergence, where great earthquakes ($M > 8$) could rupture in the Sikkim, Bhutan, or Nepal Himalaya in the future (Bilham, 2019). The evidence for seismic activity recorded in these high-altitude Taboche Lake sediment cores highlights the possibility of tectonic risks, including earthquake-triggered GLF events downstream of enlarging glacial lakes in the tectonically active Mt. Everest region.

Conclusions

High-elevation areas in the Mt. Everest region are characterized by a glacial environment that is highly sensitive to climate change. Sedimentology in combination with geochronology is essential to pinpoint and bracket the signature of environmental change or tectonic force-related event beds in the study of glacial lake cores. The 58-cm-long lake core recovered from the Taboche Lake consists of sediments $\leq$1.9 mm in diameter. Sedimentology of the lake cores indicates the occurrence of warm periods in the Gokyo valley 228.5 AD $\pm$ 91.5 years and 186.5 AD $\pm$ 57.5 years/192.5 AD $\pm$ 58.5 years and periods of oscillation between colder and warmer phases 493.5 AD $\pm$ 66.5 years/574.5 AD $\pm$ 30.5 years. The post-1807 AD $\pm$ 112 years flood turbidite at the upper part of the lake deposit corresponds to the warming trend in the Himalaya following the end of the LIA.

An earthquake-triggered turbidite event could have occurred at 1270.5 AD $\pm$ 12.5 years/1124 AD $\pm$ 82 years corresponding to the timing of the great medieval earthquake ~M 8.8 of ~1100 AD (Lavé et al., 2005) or historical earthquakes in 1223 or 1255 AD (Pant, 2002). The timing of the slumping event (1807 AD $\pm$ 112 years) illustrated by folded layers in an inclined "Z"-shaped pattern lies within the time frame of the great earthquakes ($M \geq 8$) in Bhutan in 1714 AD and in Nepal in 1934 AD or the major Himalayan earthquakes ($7 \geq M < 8$) that happened in central Nepal in 1808 or 1833 AD. Understanding past earthquakes from instrumental, historical, or geological records is crucial for seismic hazard assessment in the

Himalayan region. These results of past earthquakes recorded in the Taboche Lake highlight the importance of tectonic risks, which can also trigger GLFs in this high-altitude region and subsequent flooding in downstream areas. Thus, further explorations of lakes are essential to increase the dataset of paleoearthquakes and consequently help save lives and protect infrastructure in this increasingly populous region.

Limitations of the study

The chronology of our core is critical for our interpretations of the timing of seismic events in the high alpine region. However, radiocarbon (^{14}C) dating ages—and therefore the resulting calendar ages—can be biased to older values based on the inclusion of ^{14}C-depleted carbon (e.g., by including ancient carbonates transported from higher elevation features into the lake). According to our duplicate samples and relatively linear age model, this effect does not majorly change the results presented herein because our chronology is also tied to known seismic events. Additional, although small, biases might be introduced during the analysis of grain size of core sediment samples, which were analyzed without pretreatment because we assumed a low (<5%) concentration of organic matter. While visual inspection identified no significant organic matter present, it is possible that some organic matter may have been analyzed as terrestrial grains, although the proportion is unlikely to dramatically alter our results.

Resource availability

Lead contact

Ananta Gajurel apgajurel@fulbrightmail.org.

Materials availability

There are restrictions to the availability of sediment core material because limited volume of sample was collected and governmental regulations. However, if possible, we are glad to share subsamples of the core with reasonable compensation by the requestor for its processing and shipping.

Data and code availability

All data that was generated can be found within the manuscript.

METHODS

All methods can be found in the accompanying transparent Methods supplemental file.

SUPPLEMENTAL INFORMATION

Supplemental information can be found online at https://doi.org/10.1016/j.isci.2021.102418.

ACKNOWLEDGMENTS

This research was conducted in partnership with National Geographic Society, Rolex, and Tribhuvan University, with approval from all relevant agencies of the Government of Nepal. Funding provided by National Geographic and Rolex Perpetual Planet. We also wish to thank the communities of the Khumbu Region, our climbing support team, and Shangri-La Nepal Trek. We thank the LacCore facility at the University of Minnesota for imaging and other analyses of our cores. Tri-Chandra Multiple Campus of Tribhuvan University, Kathmandu, is thanked for administrative facilities provided to the first author. Mr. Anil Ghimire and Mr. Balkrishna Shrestha from Tri-Chandra M. Campus are highly acknowledged for their gracious support during fieldwork. We also extend our gratitude to Tyler Dinley, Sam Sheline, and Freddie Wilkinson for their help during lake coring. We also acknowledge to the reviewers for their thoughtful additions to the manuscript.

Funding: This work was supported by National Geographic Society and Rolex.

AUTHOR CONTRIBUTIONS

Conceptualization, A.P.G and M.S.H; methodology, S.M., P.A.R., M.S.H., A.P.G, B.G., and A.T.; investigation, A.P.G., M.S.H., A.E.P., S.E., P.A.M., A.T., and B.G.; formal analysis, P.A.R., S.M., and M.S.H.; Data curation, P.A.R., S.M., A.P.G., B.G., and M.S.H.; writing – original draft, A.P.G.; writing – review & editing, A.P.G., M.S.H., P.A.R., A.E.P., A.T., P.A.M., A.C.E., S.E., and B.G.; resources, A.C.E., S.E.

DECLARATION OF INTERESTS

The authors declare no conflict of interest.

Received: August 3, 2020
Revised: January 18, 2021
Accepted: April 7, 2021
Published: May 21, 2021

REFERENCES

Bajracharya, S.R., and Mool, P. (2009). Glaciers, glacial lakes and glacial lake outburst floods in the Mount Everest region, Nepal. Ann. Glaciol. *50*, 81–86.

Bajracharya, S.R., Maharjan, S.B., Shrestha, F., Sherpa, T.C., Wagle, N., and Shrestha, A.B. (2020). Inventory of glacial lakes and identification of potentially dangerous glacial lakes in the Koshi, Gandaki, and Karnali river basins of Nepal, the Tibet autonomous region of China, and India. In Research Report, N. Adve, S. Thomas, and R. Chettri, eds. (ICIMOD and UNDP), pp. 1–42.

Beck, C. (2009). Late Quaternary lacustrine paleo-seismic archives in north-western Alps: examples of earthquake origin assessment of sedimentary disturbances. Earth Sci. Rev. *96*, 327–344.

Benn, D.I., Thompson, S., Gulley, J., Mertes, J., Luckman, A., and Nicholson, L. (2017). Structure and evolution of the drainage system of a Himalayan debris-covered glacier, and its relationship with patterns of mass loss. Cryosphere *11*, 2247–2264.

Benn, D.I., Wiseman, S., and Hands, K.A. (2001). Growth and drainage of supraglacial lakes on debris- mantled Ngozumpa Glacier, Khumbu Himala, Nepal. J. Glaciol. *47*, 626–638.

Benn, D.I., Bolch, T., Hands, K., Gulley, J., Luckman, A., Nicholson, L.I., Quincey, D., Thompson, S., Toumi, R., and Wiseman, S. (2012). Response of debris-covered glaciers in the Mount Everest region to recent warming, and implications for outburst flood hazards. Earth-Science Rev. *114*, 156–174.

Bilham, R. (2019). Himalayan earthquakes: a review of historical seismicity and early 21st century slip potential. In Himalayan Tectonics: A Modern Synthesis, *483*, P.J. Treloar and M.P. Searle, eds. (Geological Society, London, Special Publications), pp. 423–482.

Byers, A.C., III, Byers, E.A., McKinney, D.C., and Rounce, D.R. (2017). A field-based study of impacts of the 2015 earthquake on potentially dangerous glacial lakes in Nepal. Himalaya *37*, 26–41.

Casey, K.A., Kaab, A., and Benn, D.I. (2012). Geochemical characterization of supraglacial debris via in situ and optical remote sensing methods: a case study in Khumbu Himalaya, Nepal. Cryosphere *6*, 85–100.

DHM (2017). Observed Climate Trend Analysis of Nepal (1971–2014) (Department of Hydrology and Meteorology, Government of Nepal). https://www.dhm.gov.np.

Folk, R.L. (1980). Petrology of Sedimentary Rock (Hemphill Publishing Company).

Gajurel, A.P., Huyghe, P., France-Lanord, C., Mugnier, J.L., Upreti, B.N., and Le Fort, P. (1998). Seismites in the Kathmandu basin, Nepal. Jour. Nepal Geol. Soc. *18*, 125–134.

Ghazoui, Z., Bertrand, S., Vanneste, K., Yokoyama, Y., Nomade, J., Gajurel, A.P., and van der Beek, P.A. (2019). Potentially large post-1505 AD earthquakes in western Nepal revealed by a lake sediment record. Nat. Commun. https://doi.org/10.1038/s41467-019-10093-4.

Ghimire, M. (2004). Review of studies on glacier lake outburst floods and associated vulnerability in the Himalayas. Himalayan Rev. *35*, 49–64.

Horstmann, B. (2004). Glacial Lake Outburst Floods in Nepal and Switzerland: New Threats Due to Climate Change (Germanwatch). www.klimaausbadekampagne.de.

Hubbard, M.S. (1989). Thermo-barometric constraints on the thermal history of the main central thrust zone and the Tibetan slab, eastern Nepal Himalaya. J. Metamorph Petrol *7*, 19–30.

ICIMOD (2011). Glacial Lakes and Glacial Lake Outburst Floods in Nepal (ICIMOD). https://lib.icimod.org/record/27755.

Jackson, M., and Bilham, R. (1994). Constraints on himalayan deformation inferred from vertical velocity fields in Nepal and Tibet. J. Geophys. Res. *99*, 13897–13912.

Karki, R., Talchabhadel, R., Aalto, J., and Baidhya, S.K. (2015). New climatic classification of Nepal. Theor. Appl. Climatol. *125*, 799–808. https://doi.org/10.1007/s00704-015-1549-0.

Khadka, N., Zhang, G., and Thakuri, S. (2018). Glacial lakes in the Nepal Himalaya: Inventory and decadal dynamics (1977–2017). Remote Sens. *10*, 1913. https://doi.org/10.3390/rs10121913.

King, O., Dehecq, A., Quincey, D., and Carrivick, J. (2018). Contrasting geometric and dynamic evolution of lake and land-terminating glaciers in the central Himalaya. Glob. Planet. Change *167*, 46–60.

King, O., Quincey, D.J., Carrivick, J.L., and Rowan, A.V. (2017). Spatial variability in mass loss of glaciers in the Everest region, central Himalayas, between 2000 and 2015. Cryosphere *11*, 407–426.

Lami, A., Marchetto, A., Musazzi, S., Salerno, F., Tartari, G., Guilizzoni, P., Rogora, M., and Tartari, G.A. (2010). Chemical and biological response of two small lakes in the Khumbu Valley, Himalayas (Nepal) to short-term variability and climatic change as detected by long-term monitoring and paleolimnological methods. Hydrobiologia *648*, 189–205.

Larsen, D.J., Miller, G.H., Geirsdóttir, Á., and Thordarson, T. (2011). A 3000-year varved record of glacier activity and climate change from the proglacial lake Hvítárvatn, Iceland. Quat. Sci. Rev. *30*, 2715–2731.

Lavé, J., Yule, D., Sapkota, S., Basant, K., Madden, C., Attal, M., and Pandey, R. (2005). Evidence for a great medieval earthquake (~1100 A.D.) in the central Himalayas, Nepal. Science *307*, 1302–1305.

Li, Y., Lu, X., and Li, Y. (2017). A review on the Little ice age and factors to glacier changes in the tian Shan, central asia. In Glaciers Evolution in a Changing World, D. Godone, ed. (IntechOpen Limited), pp. 37–60. https://doi.org/10.5772/65820.

Lin, M., Kang, S., Shaheen, R., Li, C., Hsu, S.-C., and Thiemens, M.H. (2018). Atmospheric sulfur isotopic anomalies recorded at Mt. Everest across the Anthropocene. Proc. Natl. Acad. Sci. U S A *115*, 6964–6969.

Liu, M., Chen, N., Zhang, Y., and Deng, M. (2020). Glacial Lake inventory and lake outburst flood/debris flow hazard assessment after the Gorkha earthquake in the Bhote Koshi basin. Water *12*, 464. https://doi.org/10.3390/w12020464. www.mdpi.com/journal/water.

Mischke, S., Weynell, M., Zhang, C., and Wiechert, U. (2013). Spatial variability of ^{14}C reservoir effects in Tibetan Plateau lakes. Quat. Int. *313*, 147–155. https://doi.org/10.1016/j.quaint.2013.01.030.

Mool, P.K., Bajracharya, S.R., and Joshi, S.P. (2001). Inventory of Glaciers, Glacial Lakes, and Glacial Lake Outburst Floods: Monitoring and Early Warning Systems in the Hindu Kush-Himalayan Regions – Nepal (ICIMOD).

Nakashima, Y., and Komatsubara, J. (2016). Seismically induced soft-sediment deformation structures revealed by X-ray computed tomography of boring cores. Tectonophysics *683*, 138–147.

Pant, M.R. (2002). A step towards a historical seismicity of Nepal. Adarsa *2*, 29–60.

Rana, B., Shreastha, A.B., Reynolds, J.M., Aryal, R., Pokharel, A.P., and Budhathoki, K.P. (2000). Hazard assessment of the Tsho Rolpa glacier lake and ongoing remediation measures. Jour. Nepal Geol. Soc. *22*, 563–570.

Richardson, S.D., and Reynolds, M. (2000). An overview of glacial hazards in the Himalayas. Quat. Int. *65*, 31–47.

Rounce, D.R., Scott Watson, C., and McKinney, D.C. (2017). Identification of hazard and risk for glacial lakes in the Nepal Himalaya using satellite imagery from 2000–2015. Remote Sens. *9*, 654. https://doi.org/10.3390/rs9070654.

Rowan, A.V., Egholm, D.L., Quincey, D.J., and Glasser, N.F. (2015). Modelling the feedbacks between mass balance, ice flow and debris transport to predict the response to climate change of debris covered glaciers in the Himalaya. Earth Planet. Sc. Lett. *430*, 427–438.

Rowan, A.V. (2017). The 'Little Ice Age' in the Himalaya: a review of glacier advance driven by Northern Hemisphere temperature change. Holocene *27*, 292–308.

Sabatier, P., Wilhelm, B., Ficetola, G.F., Moiroux, F., Poulenard, J., Develle, A.L., Bichet, A., Chen, W., Pignol, C., Reyss, J.L., et al. (2017). 6-kyr record of flood frequency and intensity in the western Mediterranean Alps – Interplay of solar and temperature forcing. Quatern. Sci. Rev. *170*, 121–135.

Sakai, A., and Fujita, K. (2010). Formation conditions of supraglacial lakes on debris covered glaciers in the Himalaya. J. Glaciology *56*, 177–181.

Sharma, C.M., Kang, S., Zhang, Q., and Li, Q. (2012). First results on bathymetry and limnology of high-altitude lakes in the Gokyo valley, Sagarmatha (Everest) National Park, Nepal. Limnology *13*, 181–192.

Shea, J.M., Immerzeel, W.W., Wagnon, Vincent, P.,C., and Bajracharya, S. (2015). Modelling glacier change in the Everest region, Nepal Himalaya. Cryosphere *9*, 1105–1128.

Shrestha, A.B., Wake, C.P., Mayewski, P.A., and Dibb, J.E. (1999). Maximum temperature trends in the Himalaya and its vicinity: an analysis based on temperature records from Nepal for the period 1971-1994. J. Clim. *12*, 2775–2786.

Shrestha, A.B., Eriksson, M., Mool, P., Ghimire, P., Mishra, B., and Khanal, N.R. (2010). Glacial lake outburst flood risk assessment of Sun Koshi basin, Nepal. Geomatics Nat. Hazards Risk *1*, 157–169.

Sims, J.D. (1973). Earthquake-induced structures in sediments of Van Norman lake, San Fernando, California. Science *182*, 161–163.

Sims, J.D. (2012). Earthquake-induced load casts, pseudonodules, ball-and-pillow structures, and convolute lamination: additional deformation structures for paleoseismic studies. In Recent Advances in North American Paleoseismology and Neotectonics East of the Rockies, R.T. Cox, M.P. Tuttle, O.S. Boyd, and J. Locat, eds. (Geological Society of America), pp. 191–201. https://doi.org/10.1130/2012.2493(09).

Somos-Valenzuela, M.A., McKinney, D.C., Byers, A.C., Rounce, D.R., Portocarrero, C., and Lamsal, D. (2015). Assessing downstream flood impacts due to a potential GLOF from Imja Tsho in Nepal. Hydrol. Earth Syst. Sci. *19*, 1401–1412.

Stow, D.A.V., and Shanmugam, G. (1980). Sequence of structures in fine-grained turbidites: comparison of recent deep-sea and ancient flysch sediments. Sediment. Geol. *25*, 23–42.

Survey Department. (1996). Namche Bazar. Sheet No. 278603 at 1:50000 (His Majesty's Government of Nepal).

Vandekerkhove, E., van Daele, M., Praet, N., Cnudde, V., Haeussler, P.J., and De Batist, M. (2020). Flood-triggered versus earthquake-triggered turbidites: a sedimentological study in clastic lake sediments (Eklutna Lake, Alaska). Sedimentology *67*, 364–389.

Vanniere, B., Magny, M., Joannin, S., Simonneau, A., Wirth, S.B., Hamann, Y., Chapron, E., Gilli, A., Desmet, M., and Anselmetti, F.S. (2013). Orbital changes, variation in solar activity and increased anthropogenic activities: controls on the Holocene flood frequency in the Lake Ledro area, northern Italy. Clim. Past *9*, 1193–1209.

Vuichard, D., and Zimmermann, M. (1986). The langmoche flash-flood, Khumbu Himal, Nepal. Mountain Res. Dev. *6*, 90–94.

Zheng, G., Wang, H., Wright, T.J., Lou, Y., Zhang, R., Zhang, W., and Wei, N. (2017). Crustal deformation in the India–Eurasia collision zone from 25 years of GPS measurements. J. Geophys. Res. Solid Earth *122*, 9290–9312. https://doi.org/10.1002/2017JB014465.

iScience, Volume *24*

Supplemental information

Climatic and tectonic significance of Taboche Lake, Khumbu Region, Nepal

Ananta P. Gajurel, Mary S. Hubbard, Bibek Giri, Aurora C. Elmore, Sanjeet Maka, Patrick A. Rafter, Aaron E. Putnam, Sandra Elvin, Alex Tait, and Paul A. Mayewski

Transparent Methods

Sample Collection:

In April and May 2019, as part of National Geographic and Rolex's Perpetual Planet Everest Expedition, two lake cores were recovered from the sediment-water interface from Taboche Lake, NGS-GK-219-1A (27.94289 °N, 86.698232 °E) and NGS-GK-219-1B (27.941853 °N, 86.698747 °E) (Figure 1). The cores were collected using a 5 cm diameter Unicorer; a gravity-based percussion corer with a manual hammer attachment, deployed from a temporarily-constructed catamaran made from inflatable boats (for details on the coring platform, please see Elvin et al., 2020). Immediately after core recovery in 1 m-long, clear plexiglass core tubes, the bottom of the cores were capped with a premade plastic cap and sealed with strong tape. Cores were then held upright to ensure no external contamination and no disturbance of the layered sediments. The cores were promptly transported to the lakeshore, where empty space at the top of each core tube was filled with a clean desiccant, and the top of the core barrel was sealed with a pre-made cap and taped for preservation and shipment. Due to the well preserved laminar sediments within the cores once they were opened for analysis, our core collection methods have properly preserved the internal sedimentary structures.

Firstly, a 58 cm-long core (NGS-GK-219-1A) was recovered at a distance of 95 m offshore from a 19 m-deep part of the lake (Figure 3). The second, a 56.2 cm long core (NGS-GK-219-1B), was recovered 158 m from shore, to the southeast of NGS-GK-219-1A, and a depth of 25 m (Figure 3). Because of surface freezing toward the center of the lake, core sampling in the lake's center was not possible during our field season. Though both cores came from the northern end of Taboche Lake, there were some structural differences including the fact that NGS-GK-219-1A has a significant fold in the layers of the core. Methodologies for CT scan, ^{14}C dating, and grain size analysis of these lake core sediments performed for this research are described below.

Core Scanning:

Computerized tomography scans of core NGS-GK-219-1A was performed at the University of Texas, USA. This rotate-only scan was conducted prior to the splitting of the core and provided a three dimensional view of the core's internal structure, according to the methods outlined in Orsi et al. (1994).

Radiocarbon Dating:

Radiocarbon (^{14}C) dating of one cm^3 sediment samples taken from six depth horizons in core NGS-GK-219-1A were performed at the University of California, Irvine. For each sample, the bulk lake sediment was first sealed in a quartz tube with copper (II) oxide (CuO) and silver wire, and then combusted at 900 °C for 3 hours. Samples were graphitized following Santos et al. (2007) and analyzed at the Keck Carbon Cycle Accelerator Mass Spectrometry (KCCAMS) laboratory at the University of California, Irvine (Southon et al., 2004) Sample preparation backgrounds are subtracted, based on measurements of ^{14}C-free wood. All results are corrected for isotopic fractionation according to the conventions of Stuiver and Polach (1977). Before present (BP) ages of the samples were calibrated using OxCal 4.3 (122) (2020) for corresponding age in calendar years as AD. Four of the

six sample depths were also analyzed a second time to ensure accuracy; for these duplicate samples, we are reporting both ages for the sake of clarity and transparency.

Grain Size Analysis:

Grain size of core sediments from 16 discrete samples from the second Taboche Lake core, NGS-GK-219-1B, were analyzed at the Hydro-Lab, Nepal using a laser diffraction technique using the Model Beckman Coulter LS l3320. Classification of grain size includes sand (particle diameter between 0.062 and 2 mm), silt (from 0.002 to 0.062 mm) and clay (< 0.002 mm). Samples were also observed under a binocular microscope to characterize grain size distribution (Figure 3).

Supplemental Table

Table S1. Grain size data of the second Taboche Lake core (NGS-GK-219-1B). Grain sizes were obtained using laser diffraction technique, as described in the Experimental Procedures, related to Figure 5.

Sample depth (cm)	Sand (%)	Silt (%)	Clay (%)
0.4	61.3	36.9	1.9
1.2	34.5	62.2	3.3
7.1	37.8	59.3	2.9
7.6	33.8	62.9	3.3
10.3	61.3	36.9	1.9
16.8	93.5	5.9	0.6
18.2	76.5	21.8	1.7
23.6	95.0	4.2	0.8
24.7	84.3	14.6	1.1
25.9	29.5	65.0	5.5
29.9	45.9	51.8	2.3
33.9	47.7	49.9	2.4
35.3	78.1	20.8	1.0
42.2	72.0	26.5	1.5
50.4	91.2	8.3	0.5
53.2	93.1	6.5	0.4